ACS APPLIED MATERIALS & INTERFACES

www.acsami.org

Research Article

(Macro)Molecular Imprinting of Proteins on PCL Electrospun Scaffolds

Victor Perez-Puyana, Paul Wieringa, Antonio Guerrero, Alberto Romero, and Lorenzo Moroni*

Cite This: *ACS Appl. Mater. Interfaces* 2021, 13, 29293–29302

Read Online

ACCESS | Metrics & More | Article Recommendations | Supporting Information

ABSTRACT: Biological recognition sites are very useful for biomedical purposes and, more specifically, for polymeric scaffolds. However, synthetic polymers are not capable of providing specific biological recognition sites. To solve this inconvenience, functionalization of biological moieties is typically performed, oftentimes via peptide binding. In this sense, the main task is capturing the biological complexity of a protein. This study proposes a possible alternative solution to this challenge. Our approach is based on the combination of molecular imprinting (MI) and electrospinning processes. We propose here an alternative MI approach with polymeric structures, instead of using cross-linkers and monomers as conventionally performed. Different PCL−protein scaffolds were produced via electrospinning before performing MI. Gelatin, collagen, and elastin were used as proteins. Results evidenced that the MI process conducted with PCL electrospun membranes was carried out with ionic interactions between the desired molecules and the recognition sites formed. In addition, it has been proved that MI was more efficient when using gelatin as a template. This approach opens a new stage in the development of recognition sites in scaffolds obtained with synthetic polymers and their application for biomedical purposes.

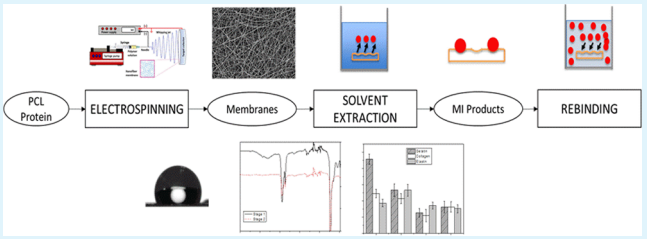

KEYWORDS: *PCL, protein, electrospinning, molecular imprinting, template*

1. INTRODUCTION

Molecular recognition is a fundamental process for the rapid recognition of enzymes and nucleic acids.[1] A biological recognition element, also called a bioreceptor, is a biological element (e.g., enzyme and antibody) sensitive to recognizing a specific analyte (e.g., enzyme substrate and antigen). It is essential to be specifically sensitive toward the specific target to prevent interference by other types of substances or signals from the surrounding matrix in a biological (micro)-environment.[2] Nowadays, polymer nanostructures are being used in the fabrication of bioreceptors due to their porous structures and larger surface areas (as in the case of nanotubes and nanofibers).[3] Specifically, synthetic polymers are highly used in material science since they allow easy control of the properties of the desired product, ensuring a high reproducibility. This quality makes them an excellent raw material in several processing techniques related to biomedical applications.[4] However, considering biomedical purposes, one of their drawbacks is the inability of providing specific biological recognition sites.

Molecular Imprinting (MI) is shown as a possible solution to solve this drawback. MI is a technique that allows the production of structures with desired biosensing properties. This technique is based on the construction of ligand-selective recognition sites in specific parts of a molecule or a structure where a template is employed as a shaper during the polymerization process.[5] The template is subsequently removed to allow the formation of vacancies with selective recognition.[6,7] A typical MI process contains a solvent, a target molecule, and a template. The solvent is generally used as dispersion media and a recognition-site-forming agent. The second element of the MI process is the target. Its main role is to form a complex with the template, thus it is necessary to select a suitable target and process to form the previous target−template complex.

There are different types of MI processes.[8] The most commonly used are the covalent and the noncovalent interactions, produced through a covalent bond or hydrogen bonding, respectively. There are also other types of interactions based on electrostatic or ionic interactions and ligand−metal coordination, which are called ionic and metal center coordination MI, respectively.[5] Most of the studies have been traditionally performed using small molecules as templates.[1,9,10]

During the MI process, the removal of the template leaves a cavity, matching the physical and chemical characteristics of the template species. Any variation from the structure of the

Received: March 5, 2021
Accepted: June 2, 2021
Published: June 15, 2021

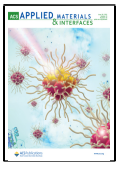

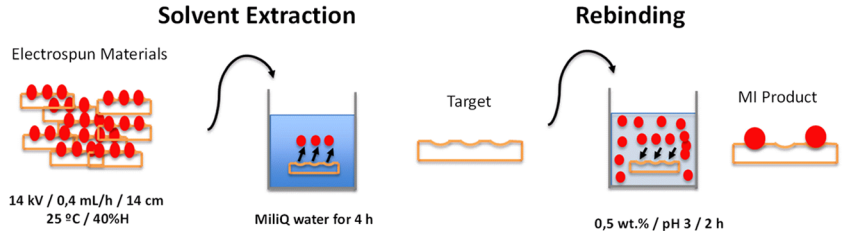

Figure 1. Schematic view of the overall molecular imprinting process.

desired species to a structurally similar, but nonidentical, entity may result in loss of selectivity. Template removal can be carried out in two different ways depending on the method used for the elimination of the template molecule in this stage, either with a simple solvent extraction or through chemical cleavage if a covalent process takes place.[11] In covalent MI, all of the recognition sites have theoretically the same affinity and selectivity due to the identical depths and shapes of the binding cavities. However, covalent MI is a less flexible method since only a few molecules can be used with a chemical condensation reaction.[12] On the other hand, although the noncovalent approach is characterized by a more heterogeneous binding, leading to a significant decrease in overall recognition performance, the removal of the template is more straightforward. This fact, combined with the different noncovalent interactions that can be performed (e.g., ionic interactions and hydrogen bonding), has made this process more popular.[13]

Traditionally, the MI process has been carried out with monomers and cross-linkers through a prepolymerization stage. However, MI can be obtained directly from polymers instead of combining monomers and cross-linkers. This new concept is called "alternative molecular imprinting" and was proposed by Yoshikawa in the late 90s.[14] It is similar to the traditional MI process, with the only difference of using polymers as the starting materials instead of monomers.[15] In this sense, our approach is based on the combined use of electrospun polymeric substrates with a solvent extraction stage. The combination of MI together with electrospinning has been previously studied but using small peptides and carrying out a chemical cleavage,[11,16−20] hindering the overall process due to the presence of additional steps involving chemical reactions.

Recent studies involved the use of different polymers for MI.[21,22] In fact, some authors presented different MI products for different purposes, such as food applications, enzyme degradation, or amino acid-specific recognition.[23−25] In this sense, the main novelty of our work is the combined use of synthetic polymers with natural polymers to develop MI products with specific sites for biological recognition. Only a few studies have combined these two techniques since the use of proteins and other biomacromolecules still poses an important challenge.[26]

Thus, our main objective was the development of an MI technique to modify electrospun scaffolds to modulate their structures and properties using proteins (macromolecular imprinting). This study considered a combination of a synthetic and a natural polymer when combining MI with electrospinning. Poly(ε-caprolactone) (PCL) was selected as a synthetic polymer due to its biocompatibility and easy processing.[27,28] Among the possible natural polymers to be selected, three different proteins (gelatin, collagen, and elastin) were analyzed and compared in terms of the efficiency of the overall process. Our hypothesis proposes the combination of the electrospinning process together with a solvent extraction step to induce the formation of specific sites in the target for the desired polymer.

2. MATERIAL AND METHODS

2.1. Materials. Gelatin protein (gelatin type B, 80−120 g Bloom) was supplied by Henan Boom Gelatin Co. Ltd. (China). In addition, type I pork collagen protein was supplied by Essentia Protein Solutions (Grasten, Denmark). Poly(ε-caprolactone) (PCL, M_w = 45 000 g/mol), bovine neck elastin, and 1,1,1,3,3,3-hexafluoro-2-propanol (HFIP) were purchased from Sigma-Aldrich (Germany).

2.2. Molecular Imprinting. *2.2.1. Process.* MI products were fabricated following a two-stage process (Figure 1). First, membranes were processed via electrospinning (Fluidnatek LE-100, Bioinicia). The electrospinning process was performed using mixtures of PCL and protein (16 and 4 w/v %, respectively). The previous solution was produced with HFIP as a solvent by stirring for ca. 24 h on a magnetic stirrer at 20 °C. Then, the electrospinning process was carried out choosing the following processing conditions: a voltage of 14 kV, a flow rate of 0.4 mL/h, a needle-collector distance of 14 cm, a temperature of 25 °C, and a humidity of 40%. The membranes obtained were formed by nanofibers of PCL (target) and protein (template). The second stage consists of template removal. This step can be carried out by solvent extraction due to the different solubility characters of the polymers selected. The solvent extraction process was conducted by immersion of the scaffolds in MiliQ water for 4 h to allow the protein to be dissolved. After that, the samples were dried overnight.

Once the MI products were obtained, the MI technique was further tested with a protein rebinding stage. In general, for the different studies performed, the reference conditions for the protein rebinding were immersion in a 0.5 wt % template solution at pH 3 for 2 h.

2.2.2. Studies Performed. Better characterization and optimization of the process can be carried out by modifying the different parameters involved. In this sense, several studies have been carried out during the template (protein) rebinding stage. First, the analysis of the template was performed to evaluate the selectivity of the process with the substitution of the template used by other macromolecules (either gelatin, collagen, or elastin). In addition, the different immersion parameters were tested (pH, immersion time, and solution concentration) to explain the mechanism involved during the process. Finally, the optimization of the process was analyzed by means of the suitability of the target used, the influence of the number of cycles performed, or the inclusion of additives in the template solution for the rebinding process.

2.3. Characterization of Nanofiber Membranes. To corroborate the efficiency of the MI process, the products were characterized at each stage of the process to follow the evolution of the membranes within the process.

2.3.1. Template Binding. The analysis of the template binding was performed using a BCA kit. The BCA Protein Assay Kit (Pierce, Bonn, Germany) was used following the manufacturer's instructions: microplate procedure (10 μL of the sample/200 μL of the BCA working reagent; incubate at 37 °C for 30 min; and measure the absorbance at 562 nm). For every microplate prepared, a BSA-

https://doi.org/10.1021/acsami.1c04022
ACS Appl. Mater. Interfaces 2021, 13, 29293−29302

dilution curve consisting of eight points up to 2000 μg/mL BSA was included as a standard to check for consistency between different experiments. The results obtained correspond to the total template content in the membrane after the rebinding process.

2.3.2. Energy-Dispersive X-ray Spectroscopy (EDAX). The atomic compositions of the membrane were examined with the energy-dispersive spectroscopy capability of the SEM equipment using an EDAX Si(Li) detector and an acceleration voltage of 5 kV. The samples were covered with a Au film in a high-resolution sputter coater. Microscopy examination of scaffolds was previously performed with an XL 30 (Philips XL Series) at an acceleration voltage of 15 kV.

2.3.3. Fourier Transform Infrared Spectroscopy (FTIR). The chemical bonds were analyzed by the attenuated total reflection-FTIR (ATR-FTIR) method using an iS50 ATR-FTIR spectrophotometer (Nicolet). Different spectra were collected in the range of 4000−1500 cm^{-1}.

2.3.4. Water Contact Angle (WCA). Scaffold wettability and hydrophobicity were assessed by water contact angle (WCA) measurements using the sessile drop method (droplets with an approximate volume of 5 μL). Both WCA values of the right and left sides of the deionized water droplets were measured and the average value was calculated. The equipment used was a drop shape analyzer (Krüss).

2.3.5. Scanning Electron Microscopy (SEM). Microscopy examination of scaffolds was assessed with an XL 30 (Philips XL Series) at an acceleration voltage of 15 kV and a magnification of ×8000. The samples were fixed onto an aluminum stub with a carbon sticker and sputter-coated with gold using the 108 auto (Cressington Scientific Instruments). Digital processing software, ImageJ, was used to determine the size of the fibers.

2.3.6. Surface Roughness. Surface topography was analyzed using a three-dimensional (3D) laser scanning microscope (Keyence). The roughness was measured in terms of the surface roughness (S_a), the root-mean-square height (S_q), and the S_z/S_a ratio.

2.4. Statistical Analysis. At least three replicates were carried out for each measurement. Statistical analyses were performed with t tests and one-way analysis of variance ($p < 0.05$) using PASW Statistics for Windows (Version 18: SPSS, Chicago, IL). Standard deviations were calculated for selected parameters. Statistical differences were indicated with $*p < 0.05$.

3. RESULTS AND DISCUSSION

3.1. Preparation of the MI Products. MI is an innovative technique that has been carried out to place small molecules on surfaces with specific sites.[15] In this sense, this study is based on the analysis of the MI process of proteins conducted with nanofibrous scaffolds fabricated via electrospinning. These samples were produced with PCL and mixtures of PCL and a protein of choice. The proteins selected were gelatin, collagen, and elastin (named as PCL−gelatin, PCL−collagen, and PCL−elastin, respectively). Pure PCL membranes were also fabricated as controls.

Initially, the membranes were characterized after electrospinning (Figure S1). Figure S1A−D shows the FTIR profiles of the different systems produced (straight line). Considering the pure PCL system (Figure S1D), a characteristic sharp band was observed at 1725 cm^{-1},[29] associated with carbonyl stretching (characteristic for PCL). However, the mixed PCL−protein systems presented, apart from the peak at 1725 cm^{-1} previously mentioned, a broad area at 3300 cm^{-1} associated with N−H stretching (traditionally named as amide A signal). This signal had higher intensity for the PCL−gelatin (Figure S1A) and the PCL−collagen (Figure S1B) ones. Furthermore, two small bands at 1640−1520 cm^{-1} were also shown in these profiles, related to carbonyl stretching and C−N stretching of amides, respectively. These peaks are characteristic of proteins.[30] In addition, Figure S1E shows the contact angle values for these systems. PCL is a hydrophobic molecule, which explains the high value observed for WCA (ca. 105°), in contrast with the values obtained for the mixed systems (PCL−gelatin, PCL−collagen, and PCL−elastin), which present a more hydrophilic character (lower WCA values). This hydrophilic character was higher for the PCL−gelatin and PCL−elastin structures, with WCA values lower than 65°.

On the other hand, the surface morphology of one of the systems was also evaluated. Figure S2 shows SEM and topographical images of the PCL−gelatin system, together with measured roughness parameters (S_a, S_q, and S_z/S_a ratio). S_a expresses the difference in the height between each peak and the arithmetical mean of the surface,[31] presenting a value of 0.6 μm. Together with S_a, S_q was included as the root-mean-square value of surface topography (0.8 μm). It is included apart from the arithmetic deviation because it presents a true meaning of the surface topography statistics. The lower the S_q value, the higher the homogeneity of the surface.[32] According to the result obtained, the surface of the membranes presents a certain heterogeneity, as also shown in previous studies.[33,34] Finally, the S_z/S_a ratio was also calculated since different surfaces could have the same values for S_a but they might present differences in the topography structure.[31] The S_z/S_a ratio represents the ratio between the highest value of the surface and S_a. According to the results obtained, the surface of the PCL−gelatin fibers presented a relatively high roughness since the S_z/S_a *ratio* was ca. 12. Moreover, Table S1 shows the EDAX results for both structures. The analysis of the PCL neat sample revealed no N in its structure, whereas the PCL−gelatin presented a 3.31 ± 0.12% of N in it.

Furthermore, after the solvent extraction stage, different products were analyzed to confirm the complete removal of the template from the structures produced (Figure S1). In this stage, PCL is insoluble in water, so the properties found for the PCL neat scaffold were the same as before. However, the other proteins are water soluble, so they are popped off into the solution from the scaffold. This effect was corroborated by the different techniques used. Figure S1A−C (dash line) also exhibited the loss of the characteristic peaks for proteins (gelatin, collagen, and elastin) in the FTIR profile, showing a similar profile to the one obtained for the pure PCL system. The alteration of the composition of the scaffold was also noticeable by the variation of WCA (Figure S1C). WCA values of the PCL−gelatin, PCL−collagen, and PCL−elastin systems increased to values higher than 100°. In other words, the solvent extraction stage led to high hydrophobic systems. In conclusion, all of the proteins present in the structure (and observed in the previous section) were lost during this stage, giving rise to a structure with cavities in which the MI process could occur.

To evaluate the functionality of the obtained MI products, a rebinding process was conducted under different conditions to better characterize the MI process. The rebinding stage was carried out by immersion in a 0.5 wt % protein (template) solution at pH 3 for 2 h.

3.2. Evaluation of the Template Selectivity. The evaluation of the template selectivity during the MI process was carried out with three different proteins: gelatin, collagen, and elastin. For this study, collagen has been selected due to its similarity in the structure with gelatin, whereas elastin was picked to use a molecule with a different structure. Therefore, a joint analysis between PCL−gelatin, PCL−collagen, PCL−

https://doi.org/10.1021/acsami.1c04022
ACS Appl. Mater. Interfaces 2021, 13, 29293−29302

elastin, and pure PCL was produced to compare the different behaviors observed for each system.

Template binding calculations (Figure 2) and fiber analyses (Figure S3) after the rebinding process were carried out. Three

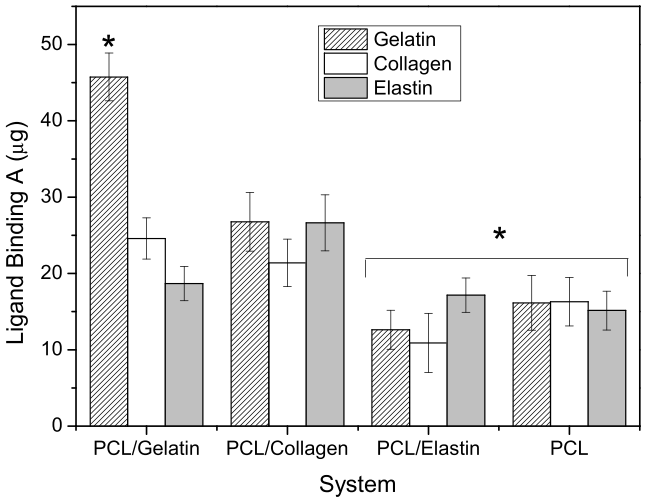

Figure 2. Template binding results obtained for PCL, PCL−gelatin, PCL−collagen, and PCL−elastin systems obtained via electrospinning after performing the rebinding stage of the MI process varying the template solution used (gelatin, collagen, or elastin). An asterisk is used to denote significant differences ($p < 0.05$). The second asterisk is spanned across PCL−elastin and PCL to mention that their values are not significantly different from each other but they are significantly lower than the other values obtained for the PCL−gelatin and PCL−collagen systems.

different effects could be observed in the template binding calculations. The membranes produced initially with PCL−gelatin showed a strong dependence on the protein used during the rebinding process. In this sense, the specific sites generated by gelatin allow a better rebinding process of proteins with a similar shape, especially if it is the same protein as what was initially used. This was verified for gelatin and collagen proteins compared to elastin. However, relatively good results were obtained for collagen as a substitute for gelatin, demonstrating the chance of using this technique to obtain scaffolds with expensive molecules from raw materials in a low concentration, using a dummy template (which can be considered gelatin). Furthermore, lower uniformity values (Table S2) were obtained during gelatin immersion compared to collagen and elastin as a consequence of possible structural modifications during the rebinding process.

On the other hand, PCL−collagen structures showed a lower rebinding efficiency than PCL−gelatin, displaying no significant differences when a different molecule than the template was used. Particularly interesting are the values obtained for collagen rebinding in PCL−collagen structures, not being significantly different than in PCL−gelatin ones, as it happened with the gelatin rebinding in PCL−gelatin systems. A possible explanation could be related to the denaturation of proteins when interacting with a hydrophobic surface such as PCL. During the rebinding, as it occurs on the surface of a molecule with a high hydrophobic character, collagen may tend to undergo a structural change induced by denaturation caused by the interaction with the PCL surface. This structural modification may be responsible for the higher protein rebinding efficiency carrying out the process with collagen on PCL−gelatin systems than on PCL−collagen ones. This structural change is also observed by the increase of the mean fiber diameter found for PCL−collagen after the rebinding process (372 nm) compared with the values found before the process (294 nm) (Table S2).

Finally, PCL−elastin and pure PCL membranes showed similar results with values of template binding in the range between 15 and 17 μg, so the efficiency of a PCL−elastin system was significantly lower compared to the other systems prepared with gelatin or collagen. This may be caused by the fact that elastin in solution tends to form interchain cross-linking with the formation of desmosine cross-linking.[35] The cross-linking that occurred in the elastin molecule may alter the protein structure and, therefore, influence the protein rebinding, consequently obtaining the low values shown in Figure 2. Interestingly, pure PCL membranes showed a higher fiber uniformity during the process (Table S2), compared to the other systems, due to their high hydrophobicity. This higher hydrophobic character makes this system more difficult to suffer changes in a protein solution.

These results reinforced the idea of the presence of a higher concentration of proteins on the surface of the PCL−gelatin and PCL−collagen membranes compared to the PCL neat scaffold after the rebinding stage. In other words, the deposition of the protein on the surface of the scaffolds is more remarkable for the systems in which protein cavities were produced (PCL−gelatin and PCL−collagen). In sum, this fact

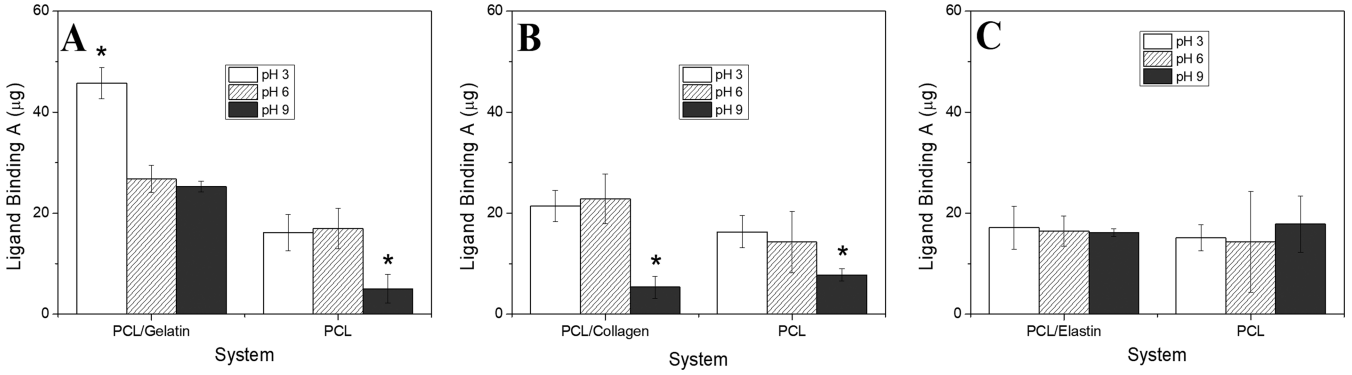

Figure 3. Template binding results obtained for (A) PCL−gelatin, (B) PCL−collagen, and (C) PCL−elastin systems obtained via electrospinning after performing the rebinding stage of the MI process varying the pH of the template solution (3, 6, or 9). The template binding results of PCL with the three templates are also included as a reference.

https://doi.org/10.1021/acsami.1c04022
ACS Appl. Mater. Interfaces 2021, 13, 29293−29302

may be explained considering that gelatin molecules (from a template solution) are inserted in some of the specific sites left by the initial gelatin after coming out during the solvent extraction stage. This effect is associated with an MI process in which there are specific sites for protein binding.

3.3. Evaluation of the Immersion Parameters. *3.3.1. Influence of the pH.* An interesting parameter to evaluate is the pH of the template solution, because it may alter the structure of the template (protein) in a solution. Three different pH were analyzed (3, 6, and 9). Figure 3A shows the ligand binding of gelatin in PCL−gelatin fibers compared to pure PCL. Two different behaviors could be seen since the PCL−gelatin system presented a ligand binding significantly higher at pH 3 compared to the ligand binding at pH 6 and pH 9. On the other hand, PCL showed similar ligand binding at pH 3 and pH 6 with a significant decrease observed at pH 9.

Figure 3B shows the results obtained for PCL−collagen and PCL. In this case, a constant deposition was observed until pH 9, when a marked decrease took place. In the case of elastin, no significant differences were observed for both systems under the pH values studied (Figure 3C).

The binding results can be explained according to the effect of pH on the different proteins studied. The isoelectric points (Ip) of gelatin and collagen proteins are at pH 4.5 and 6, respectively,[36] but the isoelectric point of elastin is at pH 10.5.[37] Thus, gelatin is positively charged at pH 3 (pH lower than the Ip) and negatively charged at pH 6 and 9 (pH higher than the Ip), whereas collagen is positively charged at pH 3, negatively charged at pH 9, and presents no net charge at pH 6 (pH similar than Ip) (Table 1). However, elastin is negatively charged at the three pH values evaluated since its Ip is higher (Table 1).

Table 1. Net Surface Charge of the Different Proteins Studied (Gelatin, Collagen, and Elastin) under Different pH Values (3, 6, and 9)

pH/protein	gelatin	collagen	elastin
pH 3	+	+	+
pH 6	−	0	+
pH 9	−	−	+

According to the results obtained, all of the proteins presented a higher protein binding when the pH was lower than the Ip, so when the proteins were positively charged. Elastin presented no significant differences since all of the studied pH values were below its isoelectric point. Taking into account that PCL is negatively charged in a solution, these results reinforced the idea of the ionic interactions between both polymers in the specific sites formed, thus highlighting a better specificity of gelatin.

3.3.2. Influence of the Immersion Time. Apart from the binding capacity, reaction kinetics for a given MIP material are a significant aspect of the MI process.[5] Thus, the immersion time of the scaffolds in the template solution during the rebinding stage was modified to study the evolution of the protein binding with time. The reference time was set at 2 h and lower and higher times were evaluated (1 and 4 h, respectively). Figure 4 shows the results for PCL−gelatin, PCL−collagen, and PCL−elastin systems at different immersion times. A similar trend was observed, with a significant increase up to 2 h of immersion time when a plateau was observed. PCL−gelatin showed the highest rebinding results, followed by PCL−collagen and PCL−elastin systems, respectively. Nevertheless, PCL showed no significant differences in the protein deposition with time, except for collagen deposition in which the values obtained at 1 h were significantly lower.

3.3.3. Influence of the Solution Concentration. Figure 5 shows the influence of the template solution concentration for the three proteins studied. PCL−gelatin meshes presented a plateau until a concentration of 0.05 wt/v %, from which a sudden decrease took place (Figure 5A). By contrast, gelatin deposition was only significantly different in PCL meshes when the concentration was 0.5%. A similar trend was observed for the PCL−collagen system in Figure 5B, with significant differences found at concentrations 0.5 and 0.05%. In this case, PCL meshes showed a nonsignificant linear decrease of collagen deposition with the decrease of the template solution concentration, being significantly lower at concentrations lower than 0.005 wt/v %. Once again, PCL−elastin and PCL meshes showed no significant differences in elastin deposition with different solution concentrations (Figure 5C).

3.4. Optimization of the MI Process. Comparing the results obtained for the different systems studied in the previous section, the system PCL−gelatin can be highlighted

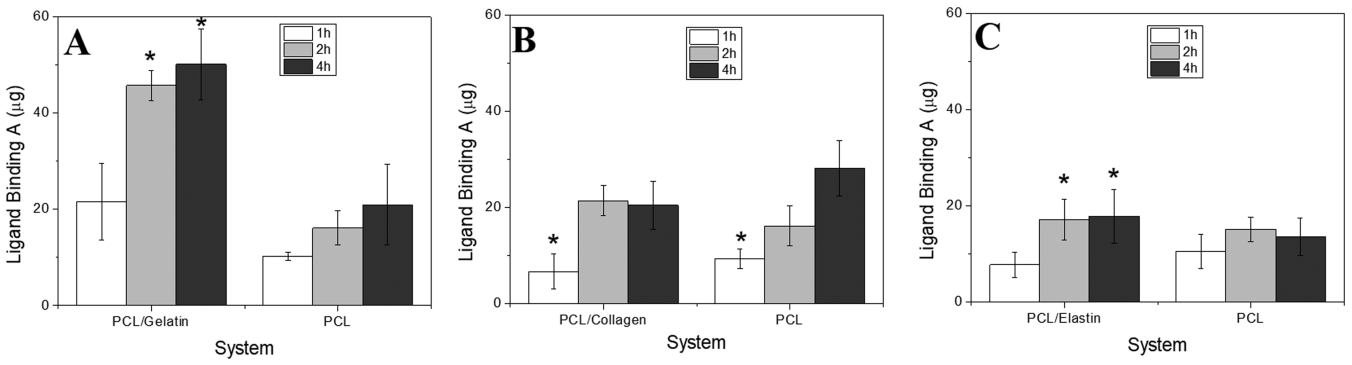

Figure 4. Template binding results obtained for (A) PCL−gelatin, (B) PCL−collagen, and (C) PCL−elastin systems obtained via electrospinning after performing the rebinding stage of the MI process varying the immersion time in the template solution (1, 2, and 4 h). The template binding results of PCL with the three templates are also included as a reference. An asterisk is used to denote significant differences ($p < 0.05$). The asterisk in (A) and (C) shows that the values at 2 and 4 h for the PCL−gelatin and PCL−elastin systems are significantly higher than all other conditions. The asterisk in (B) shows that the values at 1 h for PCL−collagen and PCL systems are significantly lower than all other conditions.

https://doi.org/10.1021/acsami.1c04022
ACS Appl. Mater. Interfaces 2021, 13, 29293−29302

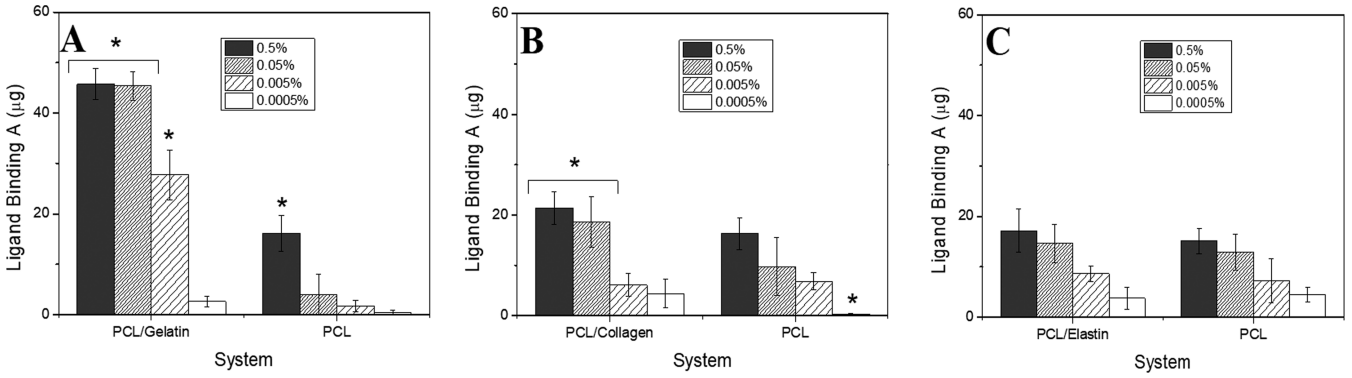

Figure 5. Template binding results obtained for (A) PCL−gelatin, (B) PCL−collagen, and (C) PCL−elastin systems obtained via electrospinning after performing the rebinding stage of the MI process varying the template solution concentration (0.5, 0.05, 0.005, and 0.0005%). The template binding results of PCL with the three templates are also included as a reference. Values with an asterisk show significant differences ($p < 0.05$). The asterisk across 0.5 and 0.05% columns for PCL−gelatin shows that their values are not significantly different from each other but they are significantly lower than the other values obtained for the PCL−gelatin and PCL meshes.

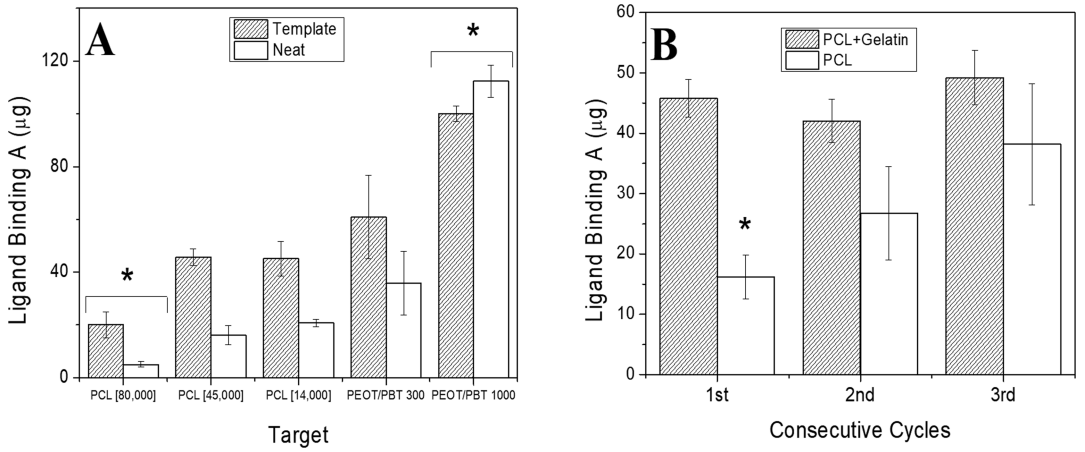

Figure 6. Template binding results obtained (A) using gelatin as a template on different targets: PCL (M_w 80 000), PCL (45 000), PCL (M_w 14 000), PEOT/PBT 300, and PEOT/PBT 1000 and (B) obtained for the PCL−gelatin system obtained via electrospinning after varying the number of consecutive rebinding cycles performed: one cycle (C1), two cycles (C2), or three cycles (C3). The template binding results of PCL are also included as a reference. An asterisk is used to denote significant differences ($p < 0.05$). The asterisk across the columns for PCL [80 000] shows that their values are significantly lower than the values obtained for the other systems. The asterisk across the columns for PEOT/PBT 1000 states that their values are significantly higher than the values obtained for the other systems.

Table 2. Ligand-Binding Ratio between the Polymer Neat and the Polymer + Gelatin Scaffold

polymer	PCL [80 000]	PCL [45 000]	PCL [14 000]	PEOT/PBT 300	PEOT/PBT 1000
Ratio	3.26	2.79	2.18	1.70	0.89

as the one which exhibits the best binding properties. Therefore, this system was selected for further analysis, which consisted of the study on the suitability of the target, the effect of successive cycles, and the effect of salts on the rebinding process (salting in/out).

3.4.1. Evaluation of the Suitability of the Target. Apart from studying the template used, the target was also analyzed. Different polymers were selected to evaluate the influence of the hydrophobicity of the target on the process (Figure 6A). Therefore, polymers with different hydrophobicities were studied by performing the process on PCL with different molecular weights (80 000, 45 000, and 14 000) and on polyethylene oxide terephthalate/polybutylene terephthalate (PEOT/PBT) copolymers. These copolymers are characterized by a random block structure and have tailorable physicochemical and mechanical properties depending on the weight ratio of the PEOT and PBT blocks as well as by the molecular weight of the initial PEG segments used in the copolymerization reaction.[38,39] They have been often used as substrates for tissue engineering and regenerative medicine applications.[40,41] Specifically, for PCL, the higher the molecular weight, the higher its hydrophobicity, whereas the PEOT/PBT copolymers are highly hydrophilic.

The differences found in the protein binding were analyzed using a ratio comparing the protein rebinding in the polymer neat scaffold and the polymer−gelatin scaffold. This ratio was calculated with the ligand-binding results obtained for the polymer−gelatin and polymer-based scaffolds according to eq 1. The results are shown in Table 2.

$$\text{ratio} = \frac{\text{ligand binding (polymer} - \text{gelatin)}}{\text{ligand binding (pure polymer)}} \quad (1)$$

https://doi.org/10.1021/acsami.1c04022
ACS Appl. Mater. Interfaces 2021, 13, 29293−29302

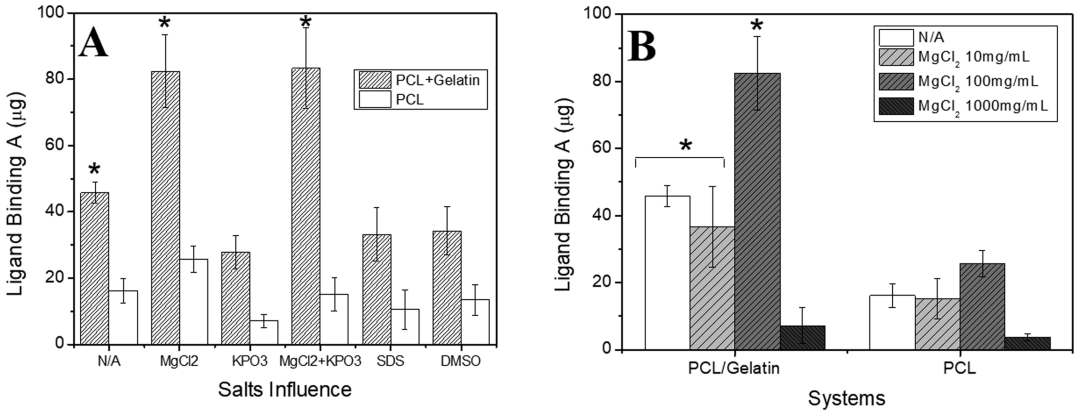

Figure 7. Template binding results obtained for the PCL−gelatin system obtained via electrospinning (A) after including different salts (10 mg/mL) during the rebinding stage of the MI process ($MgCl_2$, KPO_3, SDS, and DMSO) and (B) after including $MgCl_2$ in different concentrations (10, 100, and 1000 mg/mL). The template binding results of PCL are also included as a reference. An asterisk is used to denote significant differences ($p < 0.05$). The asterisk in Figure 7A and B shows that the values are significantly higher compared to all other conditions. The asterisk across 0.5 and 0.05% columns for PCL−gelatin (Figure 7B) shows that their values are not significantly different from each other but they are significantly different than the other values.

The ligand-binding results obtained for the different target allowed to conclude that protein binding was favored using hydrophilic polymers. However, the use of a hydrophobic polymer induced significant differences in the MI process when carrying out the process with the polymer−gelatin scaffold compared to the pure polymer system (Table 2).

3.4.2. Influence of the Number of Cycles Performed. The process was performed in successive cycles to evaluate if there was a continuous growth of the protein rebinding or the process reached a plateau. Thus, the MI process was studied after performing up to three consecutive cycles (Figure 6B). According to the template binding observed, values in the range of 45 μg were found for the PCL−gelatin system without significant differences independently of the number of cycles performed. However, PCL scaffolds showed a different behavior. An increase in the template binding was observed, evidencing an increase in protein binding when the sample was immersed in the template solution during more cycles. Gelatin binding increased from 15 ± 3 to 35 ± 4.5 μg, approximately, from the first to the third cycle. As shown in Figure 6B, this increase was significantly different from the second consecutive cycle. This effect was also observed by EDAX analysis (Table S4) with an increase in the nitrogen content (%). As discussed before, proteins tend to deposit better on hydrophilic surfaces since the interaction with hydrophobic surfaces leads to their denaturation. This could explain our results due to the fact that gelatin would occupy the same binding sites previously generated in PCL−gelatin structures, whereas the interaction of gelatin with the surface of PCL neat samples in consecutive cycles would lead to the modification of the surface, making it more hydrophilic (as shown in Figure S4 with the subsequent decrease in WCA values) and improving protein deposition. In sum, repeating this process with successive cycles (C1, C2, and C3) gave rise to similar results for the PCL−gelatin system, thus discarding the idea of traditional protein deposition.

On the other hand, WCA was also measured after performing a new solvent extraction process after the rebinding process (Figure S4). Interestingly, the contact angle reached values in the range between 95 and 105°, evidencing a marked hydrophobic character of both the PCL and PCL−gelatin systems after performing the new solvent extraction stage. The protein binding seemed to be lost after performing a solvent extraction again, evidencing the reversibility of the process.

3.4.3. Influence of the Addition of Salts. The Hofmeister series is formed by different salts with different behaviors in a solution.[42] On the one hand, there are salts that promote the salting-in effect, which is related to the stabilization of a solute in a solution (i.e., protein molecules) by decreasing the electrostatic energy between its molecules. On the other hand, there are salts that promote the salting-out effect, which consists of the precipitation of a molecule (i.e., protein) due to its favorable protein−protein interaction, leading to the formation of an aggregate, which is no longer soluble.[43]

The influence of the salting-in/out effect on the MI process was analyzed with the addition of different salts (100 mg/mL) in the template solution: magnesium chloride ($MgCl_2$), potassium phosphate (KPO_3), sodium dodecyl sulfate (SDS), and dimethyl sulfoxide (DMSO). $MgCl_2$ was used to promote the salting-in effect, whereas KPO_3 was used to promote the salting-out effect. In addition, SDS and DMSO were used to study the influence of protein folding and unfolding on the MI process. The results obtained without the addition of any salts were included as a control.

The addition of $MgCl_2$ produced a significantly higher protein rebinding compared to the control system, tested and corroborated with the template binding analysis, showing a protein rebinding 2 times higher than the reference for the PCL−gelatin system and 1.25 times higher for the PCL scaffold (Figure 7A). The salting-in effect (fomented by the addition of $MgCl_2$) promoted protein rebinding, which was more remarkable for the PCL−gelatin system.

The opposite result occurred when using KPO_3 (salting-out effect). A decrease in the template binding compared to the control (28 ± 5 μg instead of 45 ± 3 and 9 ± 2 μg instead of 18 ± 3 μg for the PCL−gelatin and PCL systems, respectively) was observed (Figure 7A). These results could be due to the fact that the salting-out effect leads to the aggregation of the protein and, therefore, the formation of big aggregates, which cannot fit in the cavities previously formed.

The influence of the combination of both effects was also studied by the immersion of the scaffolds in a template solution with $MgCl_2$, followed by the immersion in another template solution with KPO_3. The results were called $MgCl_2$ +

https://doi.org/10.1021/acsami.1c04022
ACS Appl. Mater. Interfaces 2021, 13, 29293−29302

KPO_3 (Figure 7A). In general, the template binding results showed values significantly higher than those obtained for other studies (except the ones obtained for the salting-in effect). In conclusion, once the protein rebinding occurs, the addition of salting-out molecules does not promote the subsequent release of the rebound protein.

Apart from salting-in/out salts, other substances were also evaluated to study their influence on the MI process (SDS and DMSO). Considering the results obtained in both cases, showing results similar to those obtained for salting out, a lower ligand binding was obtained comparing these values with the control ones. So, it can be concluded that a similar effect takes place when using substances promoting protein unfolding, such as SDS or DMSO.[44] Unfolding of the protein promotes its aggregation[45,46] and, subsequently, the formation of big aggregates, which cannot fit in the template cavities of the target.

The concentration of the salt can affect the salting-in/out process.[42] In this sense, different concentrations of $MgCl_2$ (10, 100, and 1000 mg/mL) were evaluated to analyze the influence of the salt concentration on the salting-in/out process (Figure 7B). No significant differences were observed when a small amount of $MgCl_2$ was included (10 mg/mL). However, a marked increase was observed when the salt concentration was higher (100 mg/mL). The improvement of the template binding was not linear with the salt concentration, as can be seen when the salt concentration was 1000 mg/mL with a dramatic decrease of the template binding. These results suggest that there is an optimal salt concentration, which enhances the salting-in effect, whereas an excessive salt concentration reverses the process, improving the salting-out effect, and thus decreasing the ligand binding.[47]

4. CONCLUSIONS

MI has been obtained by combining electrospinning with solvent extraction. The MI process here developed has been analyzed under different conditions revealing that it is a reversible process produced thanks to ionic interactions. In addition, the process presents a high selectivity, although gelatin protein can be used as a dummy template. The optimization of the process exposed that the MI process is shown to be favored when using hydrophobic targets and with the addition of substances that promote the salting-in effect. Consequently, the application of new techniques for the fabrication of biomimicking scaffolds, such as the alternative MI method here proposed, opens a new stage in the development of structures with specific biological recognition sites.

A possible approach to further characterize the MI process is the coincubation of different proteins during the rebinding process to check the preferential binding between proteins. This evaluation will be carried out in future studies, together with microscopic analyses (i.e., atomic force microscopy or transmission electron microscopy) to assess the differences found at the surface. The evaluation of the applicability will be also measured with biological studies in terms of cell adhesion and proliferation.

■ ASSOCIATED CONTENT

Supporting Information

The Supporting Information is available free of charge at https://pubs.acs.org/doi/10.1021/acsami.1c04022.

FTIR and WCA values at each MI stage, SEM and topographical analyses of the PCL/Gelatin system, SEM images after protein rebinding of the MI products in different template solutions (selectivity), WCA values at different rebinding cycles, %N content at each MI stage; the fiber diameter and uniformity of MI products before and after protein rebinding of the MI products in different template solutions, %N content for each parameter evaluated (pH, immersion time, and solution concentration), and %N content at different rebinding cycles (PDF)

■ AUTHOR INFORMATION

Corresponding Author

Lorenzo Moroni − *Department of Complex Tissue Regeneration, MERLN Institute for Technology-Inspired Regenerative Medicine, Maastricht University, 6200 MD Maastricht, The Netherlands;* orcid.org/0000-0003-1298-6025; Email: l.moroni@maastrichtuniversity.nl

Authors

Victor Perez-Puyana − *Departamento de Ingeniería Química, Universidad de Sevilla, Facultad de Química, Escuela Politécnica Superior, 41012 Sevilla, Spain; Department of Complex Tissue Regeneration, MERLN Institute for Technology-Inspired Regenerative Medicine, Maastricht University, 6200 MD Maastricht, The Netherlands*

Paul Wieringa − *Department of Complex Tissue Regeneration, MERLN Institute for Technology-Inspired Regenerative Medicine, Maastricht University, 6200 MD Maastricht, The Netherlands;* orcid.org/0000-0002-3290-5125

Antonio Guerrero − *Departamento de Ingeniería Química, Universidad de Sevilla, Facultad de Química, Escuela Politécnica Superior, 41012 Sevilla, Spain;* orcid.org/0000-0001-6050-8699

Alberto Romero − *Departamento de Ingeniería Química, Universidad de Sevilla, Facultad de Química, Escuela Politécnica Superior, 41012 Sevilla, Spain*

Complete contact information is available at: https://pubs.acs.org/10.1021/acsami.1c04022

Notes

The authors declare no competing financial interest.

■ ACKNOWLEDGMENTS

This work is part of a research project sponsored by the "Ministerio de Economía y Competitividad" (MINECO/FEDER, EU) from Spanish Government (ref CTQ2015-71164-P). The authors gratefully acknowledge their financial support. The authors also acknowledge the University of Seville for the VPPI-US grant of Victor M. Perez-Puyana. Part of this work was carried out at the Department of Complex Tissue Regeneration (MERLN Institute for Technology-Inspired Regenerative Medicine, Maastricht University) by financial support from the program *"Estancias breves en España y en el extranjero para beneficiarios de Becas predoctorales o PIF de la US y de Becas de la Fundación Cámara"* from the University of Seville. This research project was made possible by the Dutch Province of Limburg (LINK program).

REFERENCES

(1) Chen, L.; Xu, S.; Li, J. Recent Advances in Molecular Imprinting Technology: Current Status, Challenges and Highlighted Applications. *Chem. Soc. Rev.* **2011**, *40*, 2922−2942.

(2) Perumal, V.; Hashim, U. Advances in Biosensors: Principle, Architecture and Applications. *J. Appl. Biomed.* **2014**, *12*, 1−15.

(3) Ahuja, T.; Mir, I.; Kumar, D.; Rajesh. Biomolecular Immobilization on Conducting Polymers for Biosensing Applications. *Biomaterials* **2007**, *28*, 791−805.

(4) Geutjes, P. J.; Daamen, W. F.; Buma, P.; Feitz, W. F.; Faraj, K. A.; Van Kuppevelt, T. H. From Molecules to Matrix: Construction and Evaluation of Molecularly Defined Bioscaffolds. In *Tissue Engineering*; Springer: Boston, 2006; pp. 279−295.

(5) Chen, L.; Wang, X.; Lu, W.; Wu, X.; Li, J. Molecular Imprinting: Perspectives and Applications. *Chem. Soc. Rev.* **2016**, *45*, 2137−2211.

(6) Whitcombe, M. J.; Kirsch, N.; Nicholls, I. A. Molecular Imprinting Science and Technology: A Survey of the Literature for the Years 2004-2011. *J. Mol. Recognit.* **2014**, *27*, 297−401.

(7) Ye, L.; Weiss, R.; Mosbach, K. Synthesis and Characterization of Molecularly Imprinted Microspheres. *Macromolecules* **2000**, *33*, 8239−8245.

(8) Ertürk, G.; Mattiasson, B. Molecular Imprinting Techniques Used for the Preparation of Biosensors. *Sensors* **2017**, *17*, No. 288.

(9) Fasihi, J.; Ammari Allahyari, S.; Shamsipur, M.; Sharghi, H.; Charkhi, A. Adsorption of Uranyl Ion onto an Anthraquinone Based Ion-Imprinted Copolymer. *React. Funct. Polym.* **2011**, *71*, 803−808.

(10) Zhang, Z.; Li, J.; Song, X.; Ma, J.; Chen, L. Hg2+ Ion-Imprinted Polymers Sorbents Based on Dithizone−Hg2+ Chelation for Mercury Speciation Analysis in Environmental and Biological Samples. *RSC Adv.* **2014**, *4*, 46444−46453.

(11) Ghorani, B.; Tucker, N.; Yoshikawa, M. Approaches for the Assembly of Molecularly Imprinted Electrospun Nanofibre Membranes and Consequent Use in Selected Target Recognition. *Food Res. Int.* **2015**, *78*, 448−464.

(12) Turiel, E.; Martin-Esteban, A.; Fernandez, P.; Perez-Conde, C.; Camara, C. Molecular Recognition in a Propazine-Imprinted Polymer and Its Application to the Determination of Triazines in Environmental Samples. *Anal. Chem.* **2001**, *73*, 5133−5141.

(13) Wulff, G.; Schauhoff, S. Enzyme-Analog-Built Polymers. 27. Racemic Resolution of Free Sugars with Macroporous Polymers Prepared by Molecular Imprinting. Selectivity Dependence on the Arrangement of Functional Groups versus Spatial Requirements. *J. Org. Chem.* **1991**, *56*, 395−400.

(14) Yoshikawa, M.; Izumi, J.; Kitao, T.; Koya, S.; Sakamoto, S. Molecularly Imprinted Polymeric Membranes for Optical Resolution. *J. Memb. Sci.* **1995**, *108*, 171−175.

(15) Yoshikawa, M. Molecularly Imprinted Polymeric Membranes. *Bioseparation* **2001**, *10*, 277−286.

(16) Yoshikawa, M.; Tanioka, A.; Matsumoto, H. Molecularly Imprinted Nanofiber Membranes. *Curr. Opin. Chem. Eng.* **2011**, *1*, 18−26.

(17) Frenot, A.; Chronakis, I. S. Polymer Nanofibers Assembled by Electrospinning. *Curr. Opin. Colloid Interface Sci.* **2003**, *8*, 64−75.

(18) Patel, K. D.; Kim, H.; Knowles, J. C.; Poma, A. Molecularly Imprinted Polymers and Electrospinning: Manufacturing Convergence for Next-Level Applications. *Adv. Funct. Mater.* **2020**, *30*, No. 2001955.

(19) Kim, W. J.; Chang, J. Y. Molecularly Imprinted Polyimide Nanofibers Prepared by Electrospinning. *Mater. Lett.* **2011**, *65*, 1388−1391.

(20) CHE, A.; YANG, Y.; WAN, L.; WU, J.; XU, Z. Molecular Imprinting Fibrous Membranes of Poly (Acrylonitrile-Co-Acrylic Acid) Prepared by Electrospinning1. *Chem. Res. Chinese Univ.* **2006**, *22*, 390−393.

(21) de Moraes Segundo, J. d. P.; Oneide Silva de Moraes, M.; Brito, W. R.; d'Ávila, M. A. Incorporation of Molecularly Imprinted Polymer Nanoparticles in Electrospun Polycaprolactone Fibers. *Mater. Lett.* **2020**, *275*, No. 128088.

(22) Brimo, N.; Serdaroğlu, D. Ç. Molecular Imprinted Polymers for Mass Sensitive Sensors: Comparation of Performance Toward Immuno-Sensing Strategies. In *Molecular Imprinting for Nanosensors and Other Sensing Applications*; Elsevier, 2021; pp. 335−365.

(23) Ying, X.; Zhu, X.; Kang, A.; Li, X. Molecular Imprinted Electrospun Chromogenic Membrane for L-Tyrosine Specific Recognition and Visualized Detection. *Talanta* **2019**, *204*, 647−654.

(24) Li, X.; Wang, J.; Li, M.; Jin, Y.; Gu, Z.; Liu, C.; Ogino, K. Fe-Doped TiO2/SiO2 Nanofibrous Membranes with Surface Molecular Imprinted Modification for Selective Photodegradation of 4-Nitrophenol. *Chinese Chem. Lett.* **2018**, *29*, 527−530.

(25) Villa, C. C.; Sánchez, L. T.; Valencia, G. A.; Ahmed, S.; Gutiérrez, T. J. Molecularly Imprinted Polymers for Food Applications: A Review. *Trends Food Sci. Technol.* **2021**, *111*, 642−669.

(26) Li, N.; Yang, H. Construction of Natural Polymeric Imprinted Materials and Their Applications in Water Treatment: A Review. *J. Hazard. Mater.* **2021**, *403*, No. 123643.

(27) Gümüşderelioğlu, M.; Dalkıranoğlu, S.; Aydın, R. S. T.; Çakmak, S. A Novel Dermal Substitute Based on Biofunctionalized Electrospun PCL Nanofibrous Matrix. *J. Biomed. Mater. Res. Part A* **2011**, *98A*, 461−472.

(28) Woodruff, M. A.; Hutmacher, D. W. The Return of a Forgotten Polymer—Polycaprolactone in the 21st Century. *Prog. Polym. Sci.* **2010**, *35*, 1217−1256.

(29) Cebi, N.; Durak, M. Z.; Toker, O. S.; Sagdic, O.; Arici, M. An Evaluation of Fourier Transforms Infrared Spectroscopy Method for the Classification and Discrimination of Bovine, Porcine and Fish Gelatins. *Food Chem.* **2016**, *190*, 1109−1115.

(30) Muyonga, J. H.; Cole, C. G. B.; Duodu, K. G. Fourier Transform Infrared (FTIR) Spectroscopic Study of Acid Soluble Collagen and Gelatin from Skins and Bones of Young and Adult Nile Perch (Lates Niloticus). *Food Chem.* **2004**, *86*, 325−332.

(31) Tonietto, L.; Gonzaga, L.; Veronez, M. R.; Kazmierczak, C. d. S.; Arnold, D. C. M.; da Costa, C. A. New Method for Evaluating Surface Roughness Parameters Acquired by Laser Scanning. *Sci. Rep.* **2019**, *9*, No. 15038.

(32) Dong, W. P.; Sullivan, P. J.; Stout, K. J. Comprehensive Study of Parameters for Characterizing Three-Dimensional Surface Topography I: Some Inherent Properties of Parameter Variation. *Wear* **1992**, *159*, 161−171.

(33) Moghadam, B. H.; Kasaei, S.; Haghi, A. K. Surface Roughness of Electrospun Nanofibrous Mats by a Novel Image Processing Technique. *Surf. Rev. Lett.* **2019**, *26*, No. 1830005.

(34) Szewczyk, P. K.; Ura, D. P.; Metwally, S.; Knapczyk-Korczak, J.; Gajek, M.; Marzec, M. M.; Bernasik, A.; Stachewicz, U. Roughness and Fiber Fraction Dominated Wetting of Electrospun Fiber-Based Porous Meshes. *Polymers* **2018**, *11*, No. 34.

(35) Kristensen, J. H.; Karsdal, M. A. Elastin. In *Biochemistry of Collagens, Laminins and Elastin: Structure, Function and Biomarkers*; Elsevier Inc: 2016; pp 197−201.

(36) Perez-Puyana, V. M.; Jiménez-Rosado, M.; Romero, A.; Guerrero, A. Highly Porous Protein-based 3D Scaffolds with Different Collagen Concentrates for Potential Application in Tissue Engineering. *J. Appl. Polym. Sci.* **2019**, *136*, No. 47954.

(37) Foster, J. A. [30] Elastin Structure and Biosynthesis: An Overview. In *Structural and Contractile Proteins Part A: Extracellular Matrix*; Academic Press, 1982; Vol. *82*, pp. 559−570.

(38) Beumer, G. J.; van Blitterswijk, C. A.; Ponec, M. Biocompatibility of a Biodegradable Matrix Used as a Skin Substitute: An in Vivo Evaluation. *J. Biomed. Mater. Res.* **1994**, *28*, 545−552.

(39) Deschamps, A. A.; Claase, M. B.; Sleijster, W. J.; De Bruijn, J. D.; Grijpma, D. W.; Feijen, J. Design of Segmented Poly(Ether Ester) Materials and Structures for the Tissue Engineering of Bone. *J. Controlled Release* **2002**, *78*, 175−186.

(40) Wieringa, P.; Truckenmuller, R.; Micera, S.; Van Wezel, R.; Moroni, L. Tandem Electrospinning for Heterogeneous Nanofiber Patterns. *Biofabrication* **2020**, *12*, No. 025010.

https://doi.org/10.1021/acsami.1c04022
ACS Appl. Mater. Interfaces 2021, 13, 29293−29302

(41) Wieringa, P.; Girao, A.; Ahmed, M.; TruckenmÜller, R.; Welle, A.; Micera, S.; Wezel, R.; Moroni, L. A One-Step Biofunctionalization Strategy of Electrospun Scaffolds Enables Spatially Selective Presentation of Biological Cues. *Adv. Mater. Technol.* **2020**, *5*, No. 2000269.
(42) Grundl, G.; Müller, M.; Touraud, D.; Kunz, W. Salting-out and Salting-in Effects of Organic Compounds and Applications of the Salting-out Effect of Pentasodium Phytate in Different Extraction Processes. *J. Mol. Liq.* **2017**, *236*, 368−375.
(43) Hyde, A. M.; Zultanski, S. L.; Waldman, J. H.; Zhong, Y. L.; Shevlin, M.; Peng, F. General Principles and Strategies for Salting-Out Informed by the Hofmeister Series. *Org. Process Res. Dev.* **2017**, *21*, 1355−1370.
(44) Bhuyan, A. K. On the Mechanism of SDS-Induced Protein Denaturation. *Biopolymers* **2010**, *93*, 186−199.
(45) Azuaga, A. I.; Dobson, C. M.; Mateo, P. L.; Conejero-Lara, F. Unfolding and Aggregation during the Thermal Denaturation of Streptokinase. *Eur. J. Biochem.* **2002**, *269*, 4121−4133.
(46) Jahn, T. R.; Radford, S. E. Folding versus Aggregation: Polypeptide Conformations on Competing Pathways. *Arch. Biochem. Biophys.* **2008**, *469*, 100−117.
(47) Arakawa, T.; Timasheff, S. N. Mechanism of Protein Salting In and Salting Out by Divalent Cation Salts: Balance between Hydration and Salt Binding. *Biochemistry* **1984**, *23*, 5912−5923.

https://doi.org/10.1021/acsami.1c04022
ACS Appl. Mater. Interfaces 2021, 13, 29293−29302